Fabrication and characterisation of Cr and Co doped $Bi_{1.5}Zn_{0.92}Nb_{1.5}O_{6.92}$ pyrochlores

A. Mergen [a,*], H. Zorlu [a], M. Özdemir [b], M. Yumak [a]

[a] Department of Metallurgy and Materials Engineering, Marmara University, Goztepe Campus, 34722 Kadıköy, Istanbul, Turkey
[b] Marmara University, Faculty of Science and Letters, Physics Dept., Goztepe Campus, 34722 Kadıköy, Istanbul, Turkey

Available online 31 March 2011

Abstract

Cr and Co doped $Bi_{1.5}Zn_{0.92}Nb_{1.5}O_{6.92}$ pyrochlore ceramics were produced by solid state mixing of oxides. Cr and Co were doped into the Nb and Nb–Zn sites considering the compositions of $Bi_{1.5}Zn_{0.92}Nb_{1.5-x}Cr_xO_{6.92-x}$, $(Bi_{1.5}Zn_{0.46})(Zn_{0.46-3x/6}Nb_{1.5-3x/5}Cr_x)O_{6.92-x/2}$ for Cr doping and $Bi_{1.5}Zn_{0.92}Nb_{1.5-3x/5}Co_xO_{6.92}$, $(Bi_{1.5}Zn_{0.46})(Zn_{0.46-3x/6}Nb_{1.5-3x/5}Co_x)O_{6.92-x/2}$ for Co doping. The solubility limit of Cr in BZN was higher than that of Co and the solubility limit increased when doping was made both into Nb and Zn sites. The second phases appeared when $x > 0.2$ for Cr and $x > 0.15$ for Co doping into the Nb–Zn sites. Simultaneous Cr doping into the Nb- and Zn-sites of BZN pyrochlore gave higher dielectric constant than doping into the Nb-site of pyrochlore. However, Co doping into the Nb- and Zn-sites and only into the Nb-site of BZN gave identical dielectric results in the range of 202–218. The temperature coefficient of dielectric constant decreased with Cr doping and increased with Co doping.
© 2011 Elsevier Ltd. All rights reserved.

Keywords: Powders-solid state reaction; Sintering; Dielectric properties; Bismuth zinc niobate pyrochlore

1. Introduction

The general formula of a typical pyrochlore compound is $A_2B_2X_6Z$, where A and B are cations and X and Z are anions with a crystal structure belonging to a cubic system with eight formula units per unit cell.[1] The pyrochlore structure is related to a fluorite structure from which one-eighth of the anions have been removed in an ordered manner.[2] The lattice parameter ($a = 10$ Å) is approximately double that of the corresponding fluorite. Pyrochlore structures are interesting due to their ability to form substituted and defective structures. Various types of substitutions instead of A and B cations and X and Z anions have yielded numerous compounds with pyrochlore structure.[1]

Class I dielectrics, which exhibit low dielectric constants, usually under 150, have been developed for temperature stable and temperature-compensating capacitor applications. These capacitors are generally non-ferroelectrics and are characterized by a reasonable dielectric constant, a low dielectric loss and a modified temperature coefficient. One of these possible dielectric ceramics is bismuth-based pyrochlore.

Bismuth-based pyrochlores formed in the Bi_2O_3–ZnO–Nb_2O_5 system are promising materials for capacitor and high-frequency filter applications in need of temperature-stable, low-loss, high permittivity materials due to their superior dielectric properties and additional low firing capability.[3,4] Their low firing and sintering temperatures, 850–950 °C, and compatibility with Ag, allow them to be co-fired with Ag for the preparation of multilayer devices.[5,6] Although two different compositions, $Bi_{1.5}Zn_{1.0}Nb_{1.5}O_7$ and $Bi_{1.5}Zn_{0.92}Nb_{1.5}O_{6.92}$, have been given in the literature for the cubic BZN pyrochlore,[7–12] recent studies have clearly demonstrated that the exact cubic pyrochlore composition was $Bi_{1.5}Zn_{0.92}Nb_{1.5}O_{6.92}$.[7,8,13] $Bi_{1.5}Zn_{0.92}Nb_{1.5}O_{6.92}$ pyrochlore has a high permittivity ($\sim$121) and low quality factor ($Q \times f \sim 487$ GHz) at high frequency levels of 2.27 GHz.[7] This pyrochlore phase also shows dielectric relaxation between 100 and 400 K at 1.8 GHz peaking around 230 K. Dielectric relaxation may occur near room temperature at THz level frequencies.[14]

Wide range of substitutions can be made into the A and B sites of pyrochlore compounds since they have generally unusual compositional flexibility which enables to adjust the properties of pyrochlore compounds. In this context, various ions are doped into the BZN cubic pyrochlore structure to acquire materials with different dielectric properties and near to zero temperature
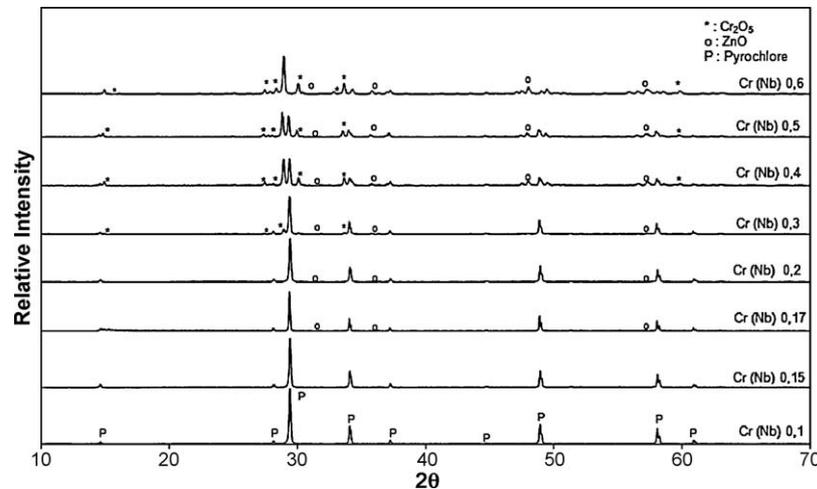
Fig. 1. XRD patterns of $Bi_{1.5}Zn_{0.92}Nb_{1.5-x}Cr_xO_{6.92-x}$ pyrochlores with different Cr dopings ($x = 0.1, 0.15, 0.17, 0.2, 0.3, 0.4, 0.5$ and 0.6).

coefficient of capacitance. In addition, additives are also used to lower the sintering temperature of BZN ceramics. 3 wt% CuO-based dopants were added into $Bi_{1.5}Zn_{0.92}Nb_{1.5}O_{6.92}$ which decreased the sintering temperature below 900 °C and increased the microwave dielectric constant to 120 at 2.3 GHz.[15] Extensive range of solid solution formation was discovered in Ti and Zr substituted $Bi_{1.5}Zn_{1.0}Nb_{1.5}O_7$. The resultant solid solutions had dielectric constants in the range of 100–200, temperature coefficients of dielectric constant −1300 ppm/K to −88 ppm/K and low dielectric loss values.[16] The introduction of Ti, Cu, Ta, Sn and Sr ions into the BZN system gave a dielectric constant in the range of 60–200, higher dielectric loss and larger negative temperature coefficient.[16–19] Sb replacing Nb in the series $(Bi_{1.8}Zn_{0.2})(Zn_{0.6}Nb_{1.4-x}Sb_x)O_7$ ($0 \leq x \leq 1.4$) decreased the dielectric constant linearly from 100 to 35, the dielectric loss kept low level ($\leq 4 \times 10^{-4}$).[20] The temperature coefficient became increasingly negative with the lowest value (−180 ppm/°C) at $x = 0.6$.

In this study, Cr and Co were doped into the $Bi_{1.5}Zn_{0.92}Nb_{1.5}O_{6.92}$ (BZN) pyrochlore where Cr and Co were introduced into B site of pyrochlore. The solubility limit of each cation was determined by X-ray diffractometer and scanning electron microscopy. The dielectric properties of doped pyrochlores were explored as a function of temperature in the frequency range of 1 kHz–2 MHz.

2. Experimental

Powder samples having the various compositions $Bi_{1.5}Zn_{0.92}Nb_{1.5-x}Cr_xO_{6.92-x}$, and $(Bi_{1.5}Zn_{0.46})(Zn_{0.46-3x/5}Nb_{1.5-3x/6}Cr_x)O_{6.92-x/2}$ for Cr doping and $Bi_{1.5}Zn_{0.92}Nb_{1.5-3x/5}Co_xO_{6.92}$ and $(Bi_{1.5}Zn_{0.46})(Zn_{0.46-3x/6}Nb_{1.5-3x/5}Co_x)O_{6.92-x/2}$ for Co doping (where $x = 0.1–0.6$) were prepared by solid state reactions using Bi_2O_3 (99.99%, Aldrich), Nb_2O_5 (99.5%, Merck), ZnO (99.5%, Aldrich), Cr_2O_3 (99%, Alfa Aesar) and Co_3O_4 (99.7%, Alfa Aesar). The constituent oxides were weighed out in proper ratios and mixed with ethyl alcohol for 15 h in a polyethylene container using zirconia milling media. Mixed powders were dried and calcined at 800 °C for 4 h. After remilling the calcined powders, they were pressed into pellets (10 mm in diameter and 2 mm in thickness) and sintered between 900 and 1050 °C for 4 h in air in a tightly closed alumina crucible to prevent
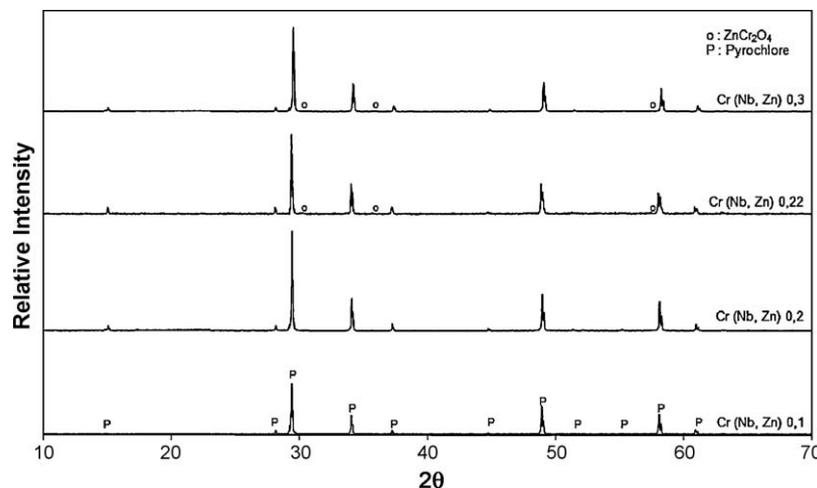

Fig. 2. XRD patterns of $(Bi_{1.5}Zn_{0.46})(Zn_{0.46-3x/6}Nb_{1.5-3x/5}Cr_x)O_{6.92-x/2}$ pyrochlores with different Cr dopings ($x = 0.1, 0.2, 0.22$ and 0.3).

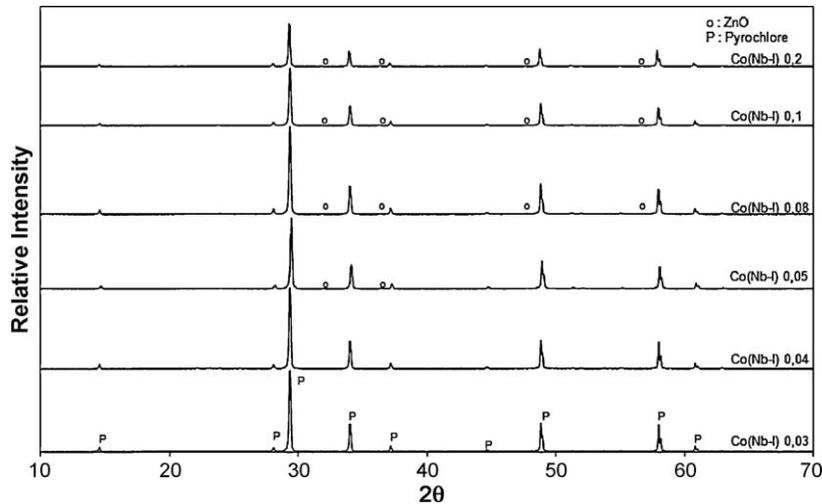Fig. 3. XRD pattern of $Bi_{1.5}Zn_{0.92}Nb_{1.5-3x/5}Co_xO_{6.92}$ pyrochlore with different Co dopings ($x = 0.03$, 0.04, 0.05, 0.08, 0.1 and 0.2).

evaporation losses. The solubility limit of Cr and Co in BZN pyrochlore and the possible second phases were determined using Rigaku X-ray diffractometer with CuKα radiation at 1°/min. Lattice parameters were refined by the least square method. The microstructural characterisation of the sintered ceramics was performed by scanning electron microscopy (JEOL JSM 5600 LV). The bulk density of the sintered samples was measured by the Archimedes method. Samples for dielectric measurements were painted electrodes with low temperature fired silver paste. An LCR meter (HP 4284A) in conjunction with a computer-interfaced temperature chamber was used in dielectric measurements in the temperature range of 20–200 °C and between frequencies of 1 kHz and 2 MHz. The temperature coefficient of dielectric constant was calculated by the following formula:

$$\alpha_\varepsilon = \frac{\varepsilon_{T_2} - \varepsilon_{T_1}}{\varepsilon_{T_1}(T_2 - T_1)}$$

where α_ε is the temperature coefficient of dielectric constant; ε_{T_2} is the dielectric constant at 120 °C; ε_{T_1} is the dielectric constant at 25 °C, $T_2 = 120$ °C and $T_1 = 25$ °C.

3. Results and discussion

3.1. XRD of Cr and Co doped BZN pyrochlores

Cr doping was made into the Nb site using the $Bi_{1.5}Zn_{0.92}Nb_{1.5-x}Cr_xO_{6.92-x}$ composition (Fig. 1). The solubility limit was $x = 0.15$ and second phases started to form when $x > 0.15$. ZnO phase (JCPDS 36-1451) formed at $x = 0.17$ and Cr_2O_5 phase (JCPDS 36-1329) started to form at $x = 0.3$. Cr was also doped into both Nb and Zn sites to increase the solubility of Cr in BZN using the composition of $(Bi_{1.5}Zn_{0.46})(Zn_{0.46-3x/6}Nb_{1.5-3x/5}Cr_x)O_{6.92-x/2}$ assuming that Zn was distributed equally into the A and B sites of BZN pyrochlore. Single phase pyrochlore was obtained when $x = 0.2$ and $ZnCr_2O_4$ phase (JCPDS 22-1107) begin to form when x

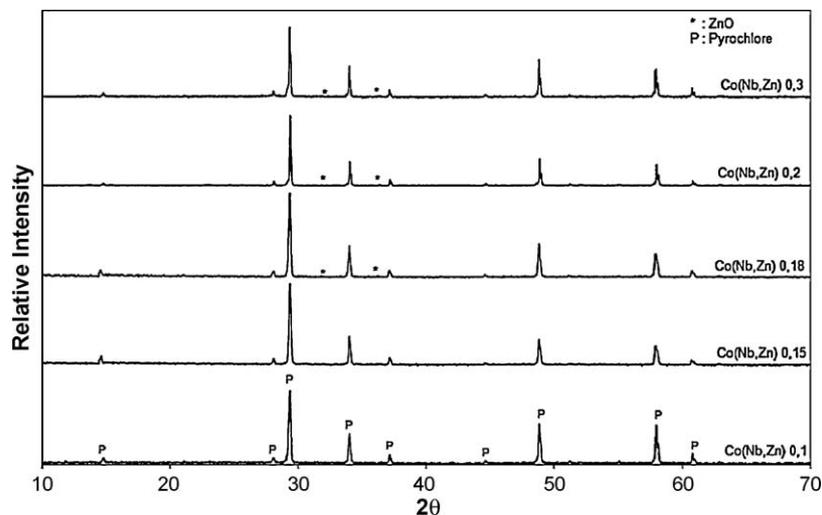Fig. 4. XRD pattern of $(Bi_{1.5}Zn_{0.46})(Zn_{0.46-3x/6}Nb_{1.5-3x/5}Co_x)O_{6.92-x/2}$ pyrochlore with different Co dopings ($x = 0.1$, 0.15, 0.18, 0.2 and 0.3).
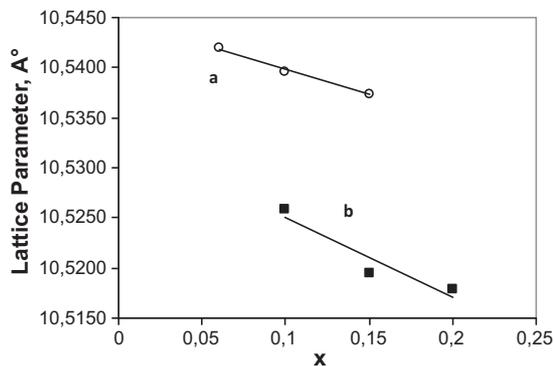
Fig. 5. Lattice parameter of Cr doped pyrochlores sintered at 1000 °C for 4 h as a function of Cr incorporation, x for (a) $Bi_{1.5}Zn_{0.92}Nb_{1.5-x}Cr_xO_{6.92-x}$ and (b) $(Bi_{1.5}Zn_{0.46})(Zn_{0.46-3x/6}Nb_{1.5-3x/5}Cr_x)O_{6.92-x/2}$.

was 0.22 (Fig. 2). These results indicated that incorporation of Cr into both Nb and Zn sites increased the solubility limit of Cr within BZN pyrochlore.

Co doping was made into the Nb site of BZN pyrochlore using the $Bi_{1.5}Zn_{0.92}Nb_{1.5-3x/5}Co_xO_{6.92}$ composition since it has identical ionic radius (0.65 Å) with Nb (0.64 Å). XRD of Co

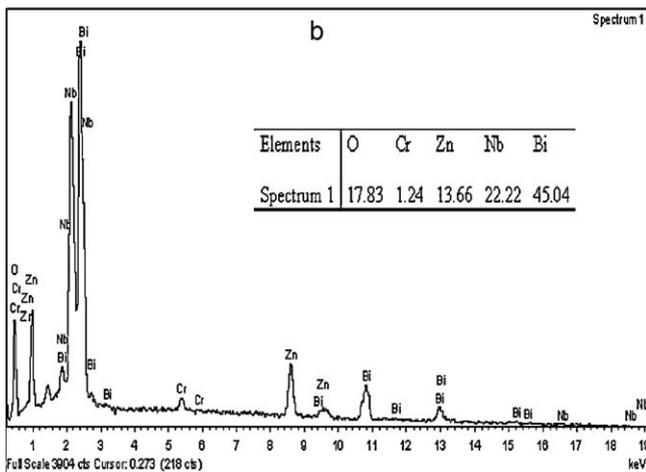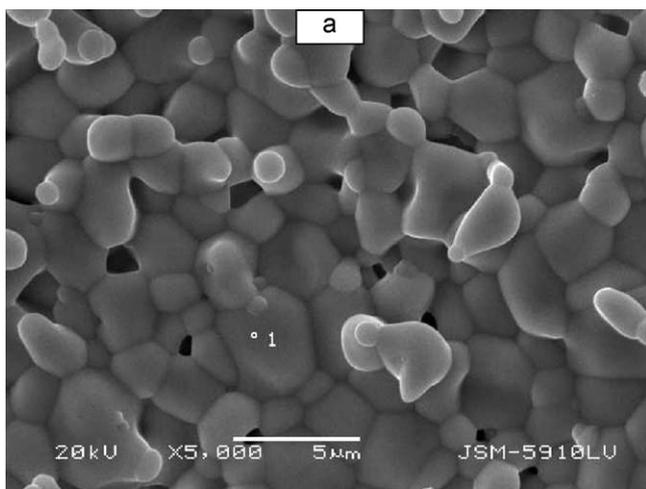| Elements	O	Cr	Zn	Nb	Bi
Spectrum 1	17.83	1.24	13.66	22.22	45.04

Fig. 6. (a) SEM micrograph and (b) EDS analysis of $Bi_{1.5}Zn_{0.92}Nb_{1.35}Cr_{0.15}O_{6.77}$ composition ($x = 0.15$) indicating single phase pyrochlore.

Table 1
The variation of lattice parameter of BZN doped with Cr and Co at different concentrations.

Phase	x	Lattice constant, Å
$Bi_{1.5}Zn_{0.92}Nb_{1.5-x}Cr_xO_{6.92-x}$	0.06	10.5417
	0.1	10.5396
	0.15	10.5374
$(Bi_{1.5}Zn_{0.46})(Zn_{0.46-3x/6}Nb_{1.5-3x/5}Cr_x)O_{6.92-x/2}$	0.1	10.5258
	0.15	10.5210
	0.2	10.5179
$Bi_{1.5}Zn_{0.92}Nb_{1.5-3x/5}Co_xO_{6.92}$	0.03	10.5386
	0.04	10.5380
$(Bi_{1.5}Zn_{0.46})(Zn_{0.46-3x/6}Nb_{1.5-3x/5}Co_x)O_{6.92-x/2}$	0.1	10.5487
	0.15	10.5536

doped BZN pyrochlore suggested that single phase pyrochlore could form only at low doping concentrations ($x \leq 0.04$). ZnO (JCPDS 36-1451) occurred as second phase when $x > 0.04$ and its content increased with x (Fig. 3). But no other phases were detected even at high concentrations of $x = 0.2$. Another composition of $(Bi_{1.5}Zn_{0.46})(Zn_{0.46-3x/6}Nb_{1.5-3x/5}Co_x)O_{6.92-x/2}$ was also used for Co doping where Co was incorporated into both Nb and Zn sites to increase its solubility limit. Co doped BZN pyrochlore sintered at 1000 °C was single phase for $x < 0.15$ and ZnO phase appeared at $x = 0.18$ indicating that the solubility limit of Co in BZN pyrochlore increased to $x = 0.15$ when Co was doped both into the Nb and Zn sites (Fig. 4).

3.2. Lattice parameters of doped BZN pyrochlores

The lattice parameters of doped single phase pyrochlores are given in Table 1. As Cr content in BZN increased, the lattice parameter of pyrochlore decreased due to smaller ionic radius of Cr (0.62 Å) than that of Nb (0.64 Å). However, the decrease in lattice parameter was higher when Cr replaced both Nb and Zn since Zn cation has larger radius (0.74 Å) than Nb. The variation of BZN lattice parameter with Cr doping, x, is linear (Fig. 5) indicating that a well behaved solid solution exists according to the Vegard's law which states that the lattice parameter of the solid solution is directly proportional to the atomic percent solute present.[21] The lattice parameters of Co doped BZN pyrochlores do not vary consistently with Co concentration (Table 1). Although Co doping into the Nb site gave identical lattice parameters, the lattice parameter slightly increased with Co in case of doping into the Nb and Zn sites due to the slightly larger ionic radius of Co (0.65 Å) than that of Nb (0.645 Å).

3.3. Microstructure of Cr doped BZN pyrochlores

The microstructure of Cr doped BZN ceramics was examined using $Bi_{1.5}Zn_{0.92}Nb_{1.5-x}Cr_xO_{6.92-x}$ composition at $x = 0.15$ (solubility limit) and $x = 0.17$ (just above the solubility limit). As suggested by XRD, the doping content of $x = 0.15$ ($Bi_{1.5}Zn_{0.92}Nb_{1.35}Cr_{0.15}O_{6.77}$) revealed only single phase pyrochlore indicating no impurity phases (Fig. 6a). EDS

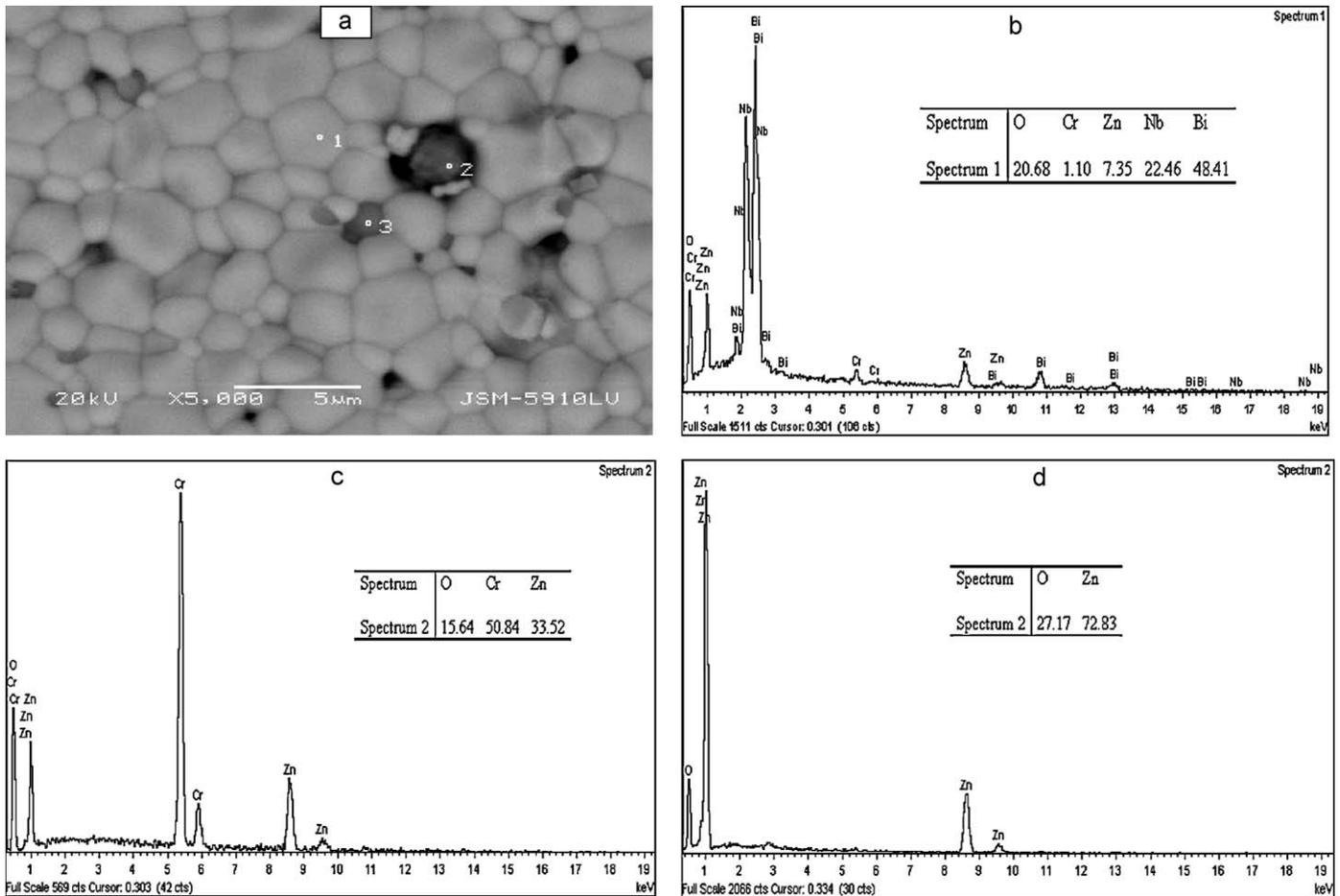Fig. 7. SEM micrograph and EDS analysis of $Bi_{1.5}Zn_{0.92}Nb_{1.33}Cr_{0.17}O_{6.75}$ composition ($x = 0.17$) (a) BEI at $\times 5.000$, (b) EDS from pyrochlore grains (point 1), (c) EDS from Cr-rich phase (point 2), and (d) EDS from ZnO phase (point 3).

analysis taken from pyrochlore grains had identical composition with theoretical values (Fig. 6b). However, SEM of higher Cr doping ($x = 0.17$; $Bi_{1.5}Zn_{0.92}Nb_{1.33}Cr_{0.17}O_{6.75}$) indicated second phases (Fig. 7). Although XRD revealed only ZnO as a second phase, Cr-rich phase was observed in addition to ZnO in SEM (Fig. 7).

3.4. Dielectric properties of Cr and Co doped BZN pyrochlores

The dielectric constant of Cr doped pyrochlore decreased with Cr doping content (Fig. 8a and b). The decrease in dielectric constant could be due lower polarizability of Cr than Nb

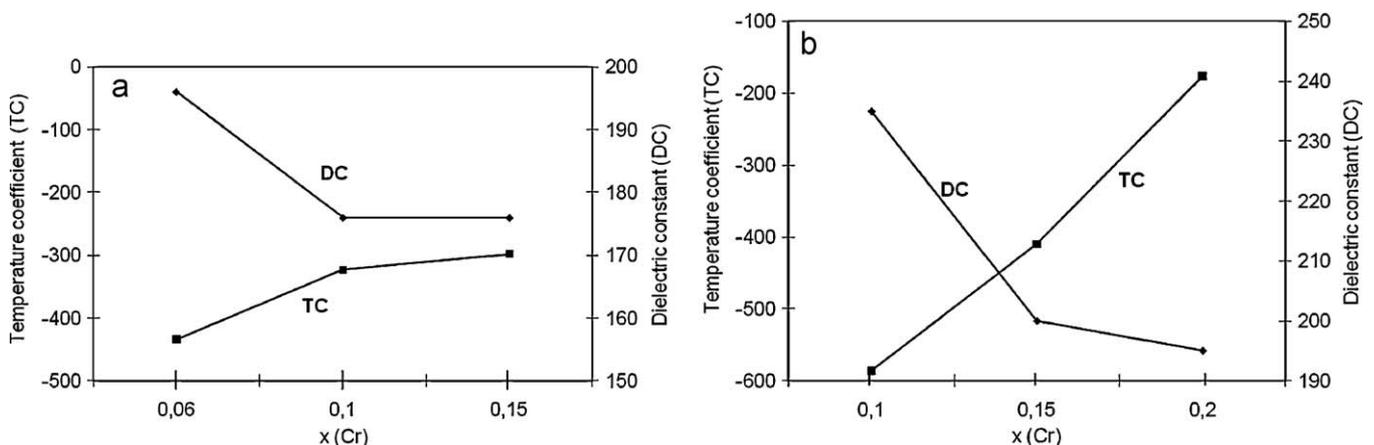Fig. 8. Variation of dielectric constant (DC) and temperature coefficient (TC) of (a) $Bi_{1.5}Zn_{0.92}Nb_{1.5-x}Cr_xO_{6.92-x}$ and (b) $(Bi_{1.5}Zn_{0.46})(Zn_{0.46-3x/6}Nb_{1.5-3x/5}Cr_x)O_{6.92-x/2}$ compositions for different Cr dopings (at 1 MHz at 25 °C).

Table 2
Dielectric properties and densities of Cr and Co doped BZN pyrochlores sintered at 1000 °C for 4 h.

	ε^a	$\tan \delta^a$	$\alpha_\varepsilon{}^b$	ρ (g/cm^3)	R_A/R_B
$Bi_{1.5}Zn_{0.92}Nb_{1.5}O_{6.92}$	178	0.0002	−647	7.04	1.662
$Bi_{1.5}Zn_{0.92}Nb_{1.5-x}Cr_xO_{6.92-x}$					
$x = 0.05$	196	0.00143	−434	6.99	1.669
$x = 0.10$	176	0.00488	−323	6.99	1.671
$x = 0.15$	176	0.00288	−298	7.09	1.672
$(Bi_{1.5}Zn_{0.46})(Zn_{0.46-3x/6}Nb_{1.5-3x/5}Cr_x)O_{6.92-x/2}$					
$x = 0.10$	235	0.00328	−586	6.99	1.685
$x = 0.15$	200	0.00081	−410	7.01	1.694
$x = 0.20$	195	0.00460	−176	7.00	1.703
$Bi_{1.5}Zn_{0.92}Nb_{1.5-3x/5}Co_xO_{6.92}$					
$x = 0.03$	205	0.00098	−488	6.99	1.667
$x = 0.04$	210	0.00160	−1212	6.89	1.667
$(Bi_{1.5}Zn_{0.46})(Zn_{0.46-3x/6}Nb_{1.5-3x/5}Co_x)O_{6.92-x/2}$					
$x = 0.10$	218	0.00103	−375	6.94	1.681
$x = 0.15$	202	0.00134	−491	7.01	1.688

[a] 20 °C at 1 MHz.
[b] 120 °C, ppm/°C ($\times 10^{-6}$).

(11.6 of Cr and 15.7 of Nb, 10^{-24} cm^3).[22] In addition, the dielectric constants of Cr doped ceramics depend on the Cr doping site. When Cr was doped into the Nb site, the dielectric constant varied between 176 and 196 but Cr doping into Zn and Nb sites resulted in higher dielectric constant values in the range of 195–235 (Table 2). This could be due to higher polarizability of Nb than Cr and lower polarizability of Zn than Cr (11.6 of Cr, 15.7 of Nb, and 7.1 of Zn, 10^{-24} cm^3). Cr doped BZN pyrochlores had large negative temperature coefficients ranging from −586 to −176 ppm/°C. In addition, Cr doping site also affects the temperature coefficient value that Cr doping into the Nb site at $x = 0.15$ and simultaneous doping into the Nb and Zn sites at $x = 0.15$ gave a temperature coefficient of −298 ppm/°C and −410 ppm/°C, respectively.

Dielectric constant, dielectric loss and temperature coefficient of Co doped BZN samples are given in Table 2. Co doping into the Nb site and simultaneous doping into the Nb and Zn sites gave identical results. In the range of compositions studied, the dielectric constant and temperature coefficient ranged from 202 to 218 and from −375 to 652 ppm/°C, respectively, with one composition having a very high temperature coefficient of $1212 \times 10^{-6}/°C$. The dielectric loss of Co doped BZN pyrochlores varied between 0.00098 and 0.00160 at 1 MHz at 25 °C depending on the Co doping concentration and Co doping site.

Valant and Davies[16] observed that a correlation exists between tolerance factor or the ratio of the A and B-site ionic radii (R_A/R_B) and the temperature coefficient (τ_K) in $(Bi_{1.5}Zn_{0.5})(Zn_{0.5}Nb_{1.5})O_7$ systems doped with Ti, Zr and Gd. But in this study controversial results were obtained. For Cr doped BZN samples, τ_K value increased with increasing R_A/R_B (Table 2). However, the τ_K values of Co doped BZN samples decreased with increasing Co doping. In the present study, ionic ratios (R_A/R_B) were calculated assuming that Zn cations
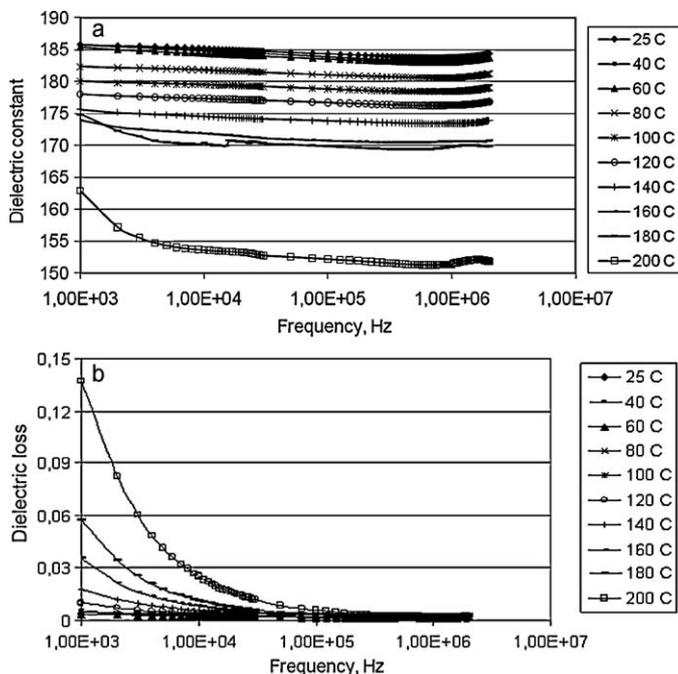

Fig. 9. Frequency and temperature dependence of (a) dielectric constant and (b) dielectric loss of Cr doped samples for $x = 0.1$ in $Bi_{1.5}Zn_{0.92}Nb_{1.5-x}Cr_xO_{6.92-x}$ composition ($Bi_{1.5}Zn_{0.92}Nb_{1.4}Cr_{0.1}O_{6.82}$).

were distributed over A and B-sites equally giving a formula of $(Bi_{1.5}Zn_{0.46})(Zn_{0.46}Nb_{1.5})O_{6.92}$.[23]

The dielectric properties of Cr and Co doped BZN ceramics at different doping concentrations indicated identical behaviour with frequency and temperature. The change of dielectric constant and dielectric loss of Cr doped $Bi_{1.5}Zn_{0.92}Nb_{1.5-x}Cr_xO_{6.92-x}$ composition for $x = 0.1$ ($Bi_{1.5}Zn_{0.92}Nb_{1.4}Cr_{0.1}O_{6.82}$) is given in Fig. 9. The dielectric constant was nearly stable with frequency below 180 °C but indicated a slight variation at 180 and 200 °C. However, the temperature had a significant effect on dielectric constant which increased with temperature. No peaks were observed in the dielectric constant–frequency curve which could be due to lattice polarization with no dipole formation.[24] The dielectric loss was high at low frequencies above 120 °C and a sharp decrease was observed above 30 kHz after which it did not change significantly with frequency. The dielectric loss was below $0.006 < 120 °C$ at all frequencies and was nearly independent of frequency. The decrease in dielectric loss with frequency is due to leakage conduction.[25,26] The dielectric loss increased significantly with temperature below 30 kHz. The rise in dielectric loss with temperature is possibly due to the increase in the number of charge carriers.[24] But no change was observed in dielectric loss with temperature above 30 kHz.

4. Conclusion

Cr and Co doped $Bi_{1.5}Zn_{0.92}Nb_{1.5}O_{6.92}$ pyrochlore ceramics were produced using various compositions where Cr and Co were doped into only Nb site and into both Nb and Zn sites of BZN. The solubility limits of Cr and Co were

higher when they were doped into both Nb and Zn sites rather than only into the Zn site. The solubility of Cr and Co was $x = 0.20$ and $x = 0.15$, respectively, along the compositions of $(Bi_{1.5}Zn_{0.46})(Zn_{0.46-3x/6}Nb_{1.5-3x/5}Cr_x)O_{6.92-x/2}$ and $(Bi_{1.5}Zn_{0.46})(Zn_{0.46-3x/6}Nb_{1.5-3x/5}Co_x)O_{6.92-x/2}$. Well-behaved solid solutions were obtained according to the Vegard's law for Cr doping. $ZnCr_2O_4$, Cr_2O_5 and ZnO second phases were detected above the solubility limits for Cr doping. Cr and Co doped BZN pyrochlores had significantly different dielectric properties than pure BZN pyrochlore. While the dielectric constant of BZN decreased with an increase in Cr doping, temperature coefficient approached to zero with Cr. Higher dielectric constants and larger temperature coefficients were obtained with higher Cr doping.

Acknowledgements

References

1. Subramanian MA, Aravamudan G, Subba Rao GV. Oxide pyrochlores—a review. *Prog Solid State Chem* 1983;**15**:55–143.
2. Aleshin E, Roy R. Crystal chemistry of pyrochlore. *J Am Ceram Soc* 1962;**45**:18–25.
3. Cann DP, Randall CA, Shrout TR. Investigation of the dielectric properties of bismuth pyrochlores. *Solid State Commun* 1996;**100**:529–34.
4. Valant M, Davies PK. Crystal chemistry and dielectric properties of chemically substituted $(Bi_{1.5}Zn_{150}Nb_{1.5})O_7$ and $Bi_2(Zn_{4/3}Nb_{4/3})O_7$ pyrochlores. *J Am Ceram Soc* 2000;**83**:147–53.
5. Nino JC, Lanagan MT, Randall CA. Phase formation and reactions in the BZN–Ag pyrochlore system. *J Mater Res* 2001;**16**:1460–4.
6. Cho SY, Youn HJ, Kim DW, Kim TG, Ban KS. Interaction of BiNbO4-based low-firing ceramics with silver electrode. *J Am Ceram Soc* 1998;**81**:3038–40.
7. Levin I, Amos TG, Nino JC, Vanderah TA, Randall CA, Lanagan MT. Structural study of an unusual cubic pyrochlore $Bi_{1.5}Zn_{0.92}Nb_{1.5}O_{6.92}$. *J Solid State Chem* 2002;**168**:69–75.
8. Wu MC, Kamba S, Bovtun V, Su WF. Comparison of microwave dielectric behavior between $Bi_{1.5}Zn_{0.92}Nb_{1.5}O_{6.92}$ and $Bi_{1.5}ZnNb_{1.5}O_7$. *J Eur Ceram Soc* 2006;**26**:1889–93.
9. Hong W, Huiling D, Xi Y. Structural study of Bi_2O_3–ZnO–Nb_2O_5 based pyrochlores. *Mater Sci Eng B* 2003;**99**:20–4.
10. Wang X, Wang H, Yao X. Structures, phase transformations, and dielectric properties of pyrochlores containing bismuth. *J Am Ceram Soc* 1997;**80**:2745–8.
11. Wang Q, Wang H, Yao X. Structure, dielectric and optical properties of $Bi_{1.5+x}ZnNb_{1.5}O_{7+1.5x}$ pyrochlores. *Ceram Int* 2009;**35**:143–6.
12. Du H, Yao X, Zhang X, Weng H. Defect structure and dielectric properties of Bi-based pyrochlores probed by positron annihilation. *Appl Surf Sci* 2006;**253**:1856–60.
13. Mergen A, Özyoldaş O. Production and dielectric properties of $Bi_{1.5}Zn_{1.0}Nb_{1.5}O_7$ and $Bi_{1.5}Zn_{0.92}Nb_{1.5}O_{6.92}$ pyrochlore ceramics. *Ceram Silicaty* 2010;**54**:31–7.
14. Withers RL, Welbury TR, Larssen AK, Liu Y, Noren L, Rundolf H, et al. Local crystal chemistry, induced strain and short range order in the cubic pyrochlore BZN. *J Solid State Chem* 2004;**177**: 231–44.
15. Wu MC, Huang YC, Su WF. Silver cofirable $Bi_{1.5}Zn_{0.92}Nb_{1.5}O_{6.92}$ microwave ceramics containing CuO-based dopants. *Mater Chem Phys* 2006;**100**:391–4.
16. Valant M, Davies PK. Crystal chemistry and dielectric properties of chemically substituted $(Bi_{1.5}Zn_{1.0}Nb_{1.5})O_7$ and $Bi_2(Zn_{2/3}Nb_{4/3})O_7$ pyrochlores. *J Am Ceram Soc* 2000;**83**:147–53.
17. Cann DP, Randall CA, Shrout TR. Dielectric relaxation and microwave dielectric properties of Bi_2O_3–ZnO–Ta_2O_5 ceramics. *Solid State Commun* 1996;**100**:529–34.
18. Du HL, Yao X. Investigation of dielectric properties of Bi_2O_3–ZnO–Nb_2O_5–Sb_2O_3 based pyrochlores. *Ferroelectrics* 2001;**262**:83–8.
19. Du HL, Yao X, Zhang LY. Structure, IR spectra and dielectric properties of Bi_2O_3–ZnO–SnO_2–Nb_2O_5 quarternary pyrochlore. *Ceram Int* 2002;**28**:231–4.
20. Du H, Yao X. Synthesis and dielectric properties development of new thermal stable bismuth pyrochlores. *J Phys Chem Solids* 2002;**63**:2123–8.
21. Cullity BD, Stock SR. *Elements of X-ray diffraction*. 3rd ed. Englewood Cliffs (NJ): Prentice Hall; 2001.
22. Shihua D, Xi Y, Li Y. Study of structure and dielectric properties of non-stoichiometric Bi_2O_3–ZnO–Nb_2O_5 ceramics. *J Electroceram* 2008;**21**:435–8.
23. Mergen A, Lee WE. Crystal chemistry, thermal expansion and dielectric properties of $(Bi_{1.5}Zn_{0.5})(Sb_{1.5}Zn_{0.5})O_7$ pyrochlore. *Mater Res Bull* 1997;**32**:175–89.
24. Nobre MAL, Lanfredi S. Dielectric properties of $Bi_3Zn_2Sb_3O_{14}$ ceramics at high temperature. *Mater Lett* 2001;**47**:362–6.
25. Wang H, Peng Z, Du H, Yao T, Yao X. Mn^{4+} & W^{6+} substitution on Bi_2O_3–ZnO–Nb_2O_5-based low firing ceramics. *Ceram Int* 2004;**30**:1219–23.
26. Lines ME, Glass AM. *Principle and applications of ferroelectric materials*. Oxford: Clarendon Press; 1977.